Supporting information

Belonging to the manuscript

Fluoride substitution in sodium hydride for thermal energy storage applications

Terry D. Humphries,* Drew A. Sheppard, Matthew R. Rowles, M. Veronica Sofianos, Craig. E. Buckley

Hydrogen Storage Research Group, Fuels and Energy Technology Institute, Curtin University, GPO Box U1987, Perth, WA 6845, Australia

E-mail: terry_humphries81@hotmail.com

Table S1. Peak positions and corresponding Miller indices of the NaH_xF_{1-x} mixtures after Ball milling and annealing determined by Rietveld refinement of the SR-XRD data. Relative peak intensities in parentheses. λ = 0.824890 Å, 27 °C.

	Peak position (2θ)					
hkl	**NaH**	**$NaH_{0.95}F_{0.05}$**	**$NaH_{0.85}F_{0.15}$**	**$NaH_{0.7}F_{0.3}$**	**$NaH_{0.5}F_{0.5}$**	**NaF**
111	16.83 (1)	16.89 (1)	17.01 (0.81)	17.24 (0.45)	17.31 (0.23)	17.74 (0.02)
002	19.46 (0.64)	19.53 (0.85)	19.66 (1)	19.94 (1)	20.01 (1)	20.51 (1)
022	27.65 (0.39)	27.75 (0.50)	27.95 (0.59)	28.34 (0.59)	28.45 (0.56)	29.16 (0.59)
311	32.55 (0.37)	32.67 (0.37)	32.90 (0.32)	33.37 (0.20)	33.49 (0.10)	34.34 (0.02)
222	34.04 (0.11)	34.16 (0.14)	34.41 (0.17)	34.90 (0.17)	35.03 (0.15)	35.91 (0.17)

Table S2. Compositions of NaH_xF_{1-x} mixtures after Ball milling and annealing determined by Rietveld refinement of the SR-XRD data. λ = 0.824890 Å, 27 °C.

Sample	**Composition (wt.%)**	
	NaH_xF_{1-x}	NaOH
NaH	88	12
$NaH_{0.95}F_{0.05}$	91.0	9.0
$NaH_{0.85}F_{0.15}$	90.5	9.5
$NaH_{0.7}F_{0.3}$	88.6	11.4
$NaH_{0.5}F_{0.5}$	96.3	3.7
NaF	100	0

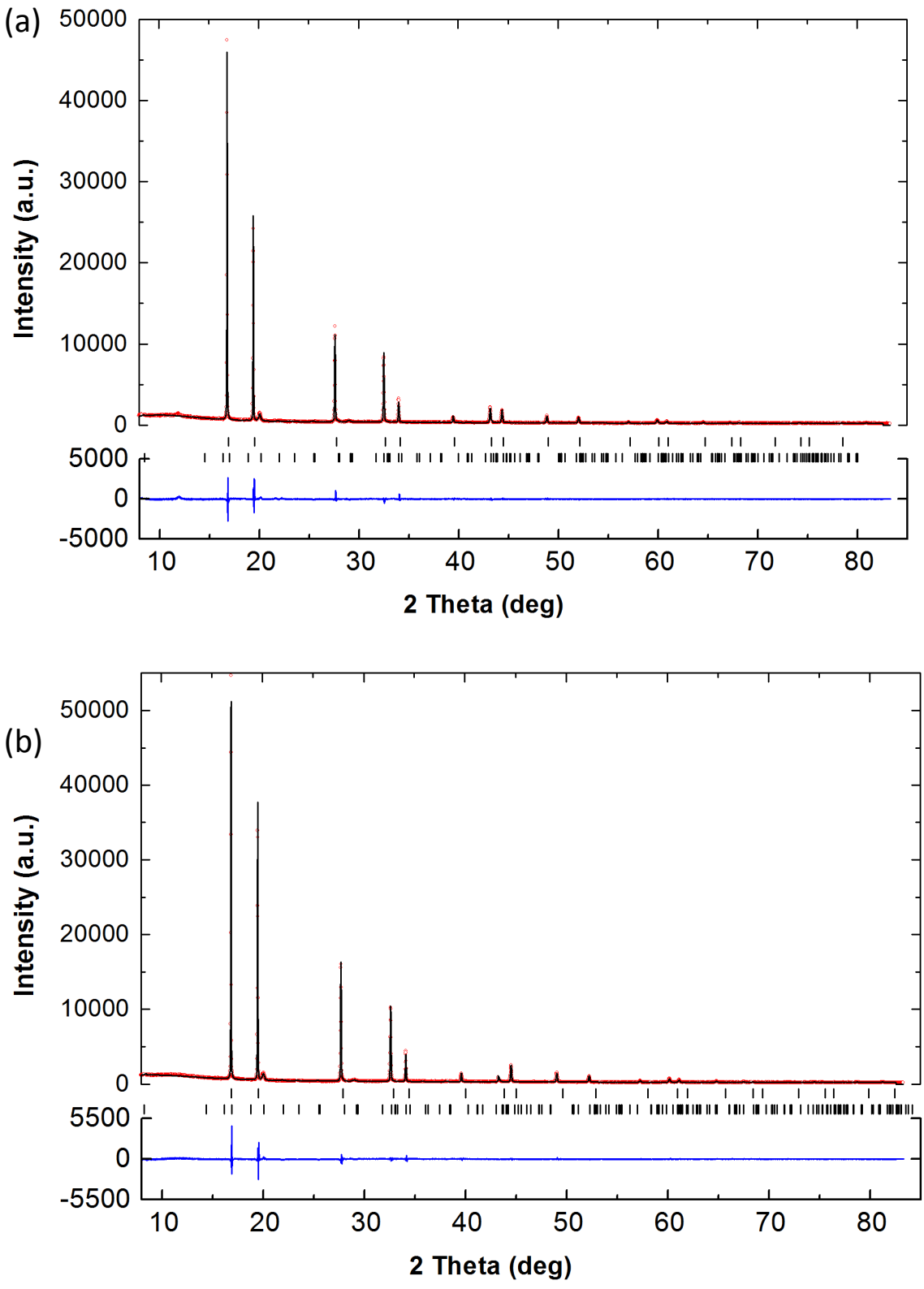
(a)
Intensity (a.u.)
50000
40000
30000
20000
10000
0
5000
0
-5000
10
20
30
40
50
60
70
80
2 Theta (deg)
(b)
Intensity (a.u.)
50000
40000
30000
20000
10000
0
5500
0
-5500
10
20
30
40
50
60
70
80
2 Theta (deg)

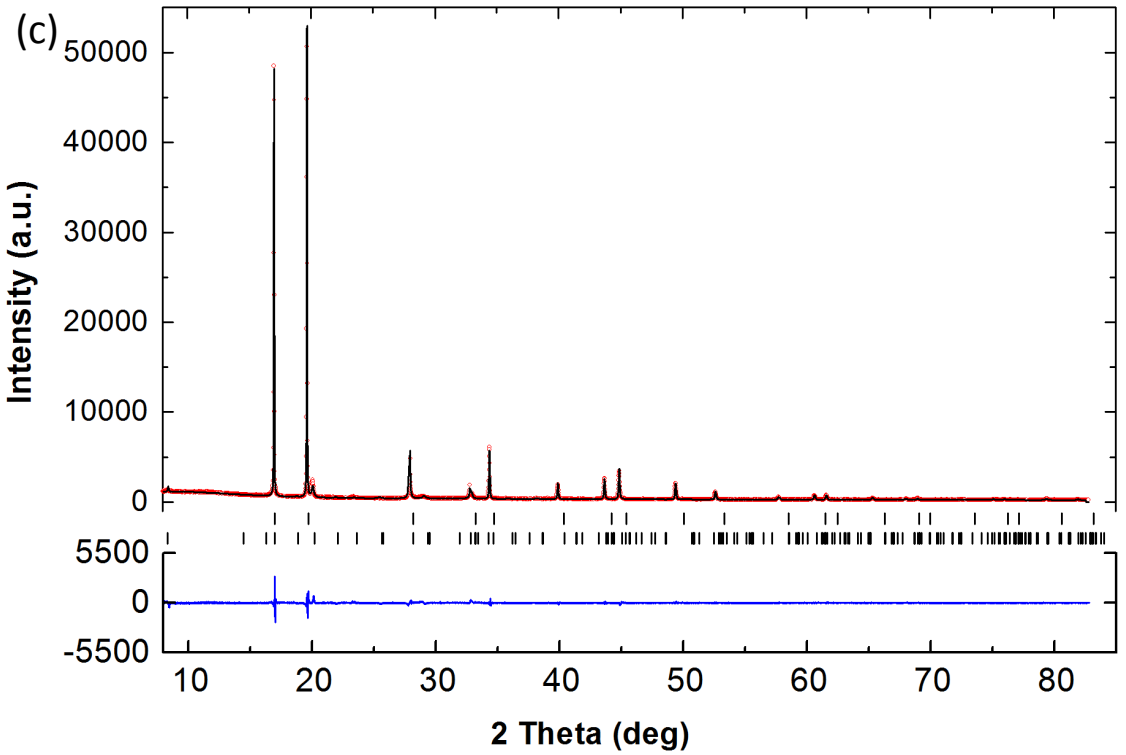
(c)
Intensity (a.u.)
50000
40000
30000
20000
10000
0
5500
0
-5500
10
20
30
40
50
60
70
80
2 Theta (deg)

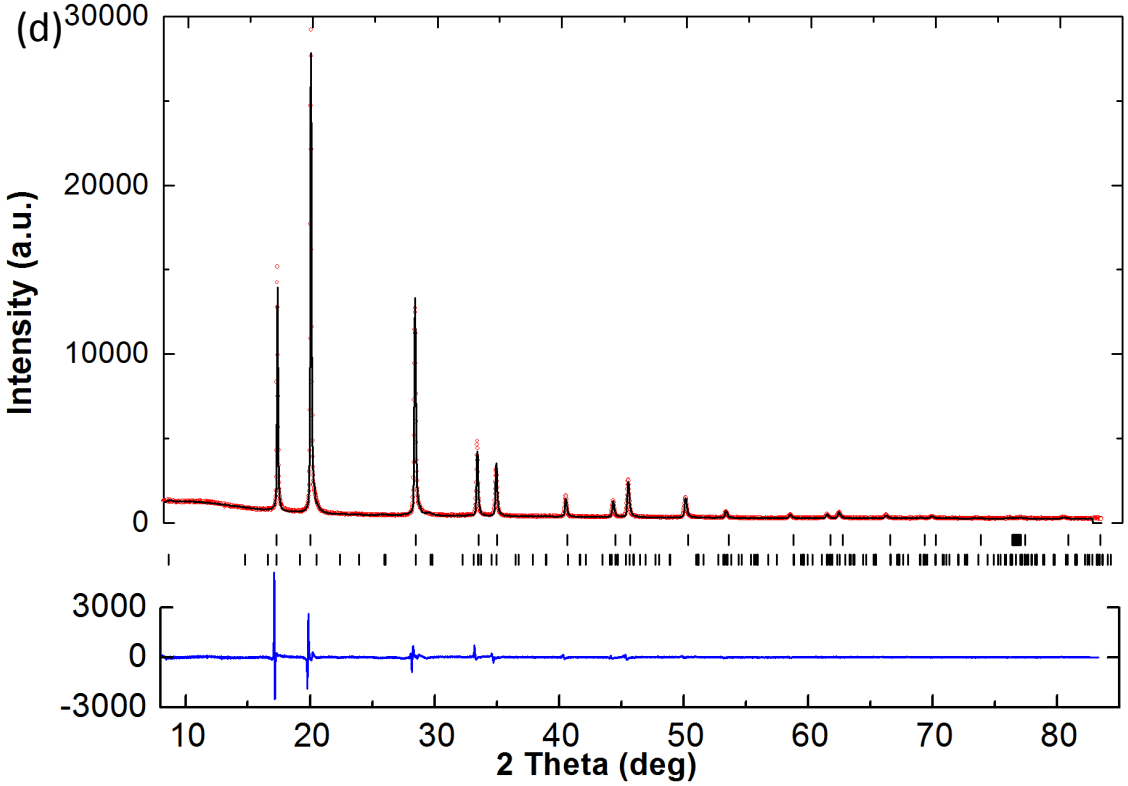
(d)
Intensity (a.u.)
30000
20000
10000
0
3000
0
-3000
10
20
30
40
50
60
70
80
2 Theta (deg)

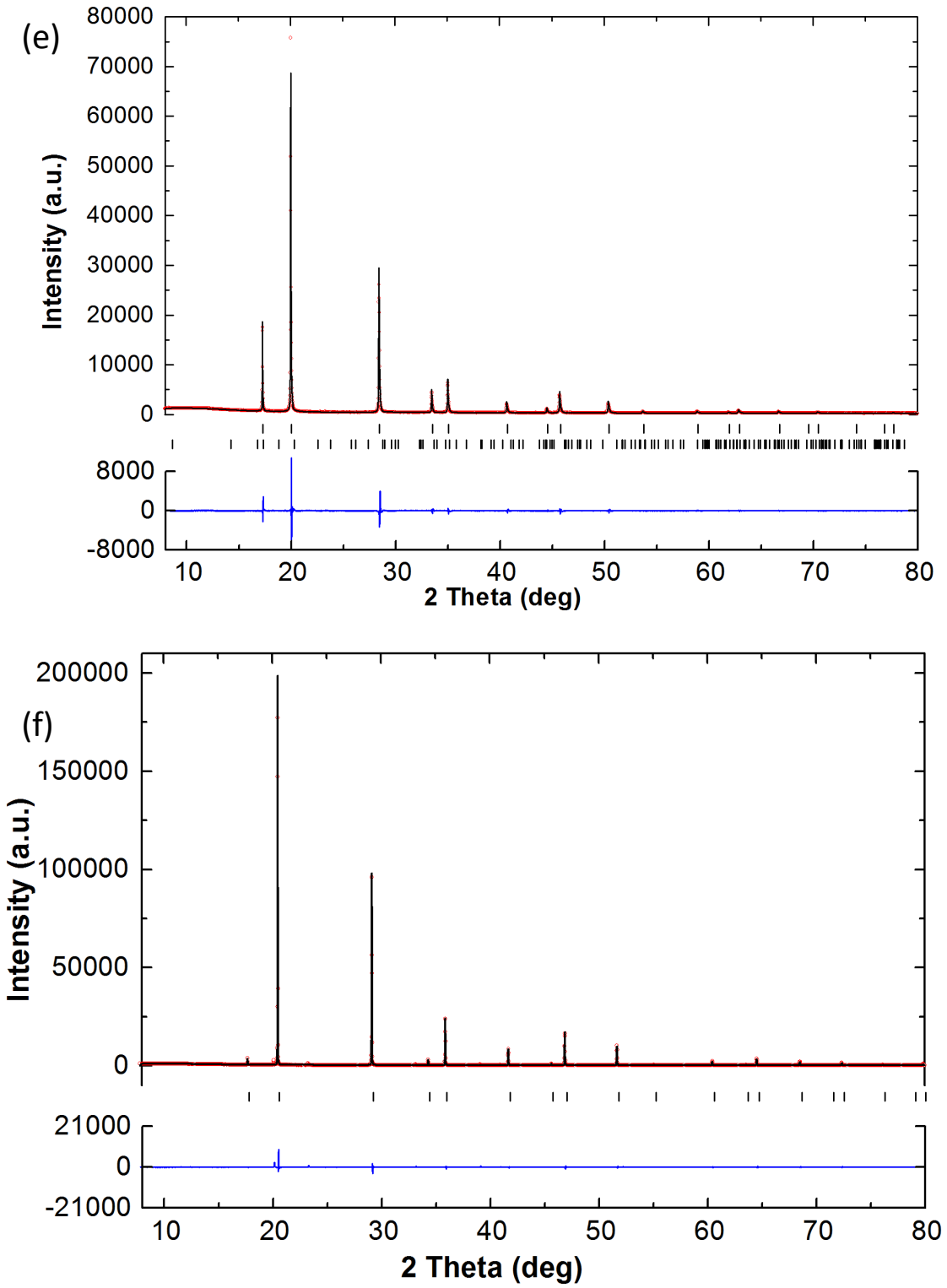

Fig. S1. Rietveld refinement plot of (a) NaH, (b) $NaH_{0.95}F_{0.05}$, (c) $NaH_{0.85}F_{0.15}$, (d) $NaH_{0.7}F_{0.3}$, (e) $NaH_{0.5}F_{0.5}$ and (f) NaF. Experimental data as red circles, calculated diffraction pattern as black line and the difference plot in blue. Tick marks show positions for: (a - e) NaH_xF_{1-x} (top) and NaOH (bottom), respectively; (f) NaF. λ = 0.824890 Å, T = 27 °C.

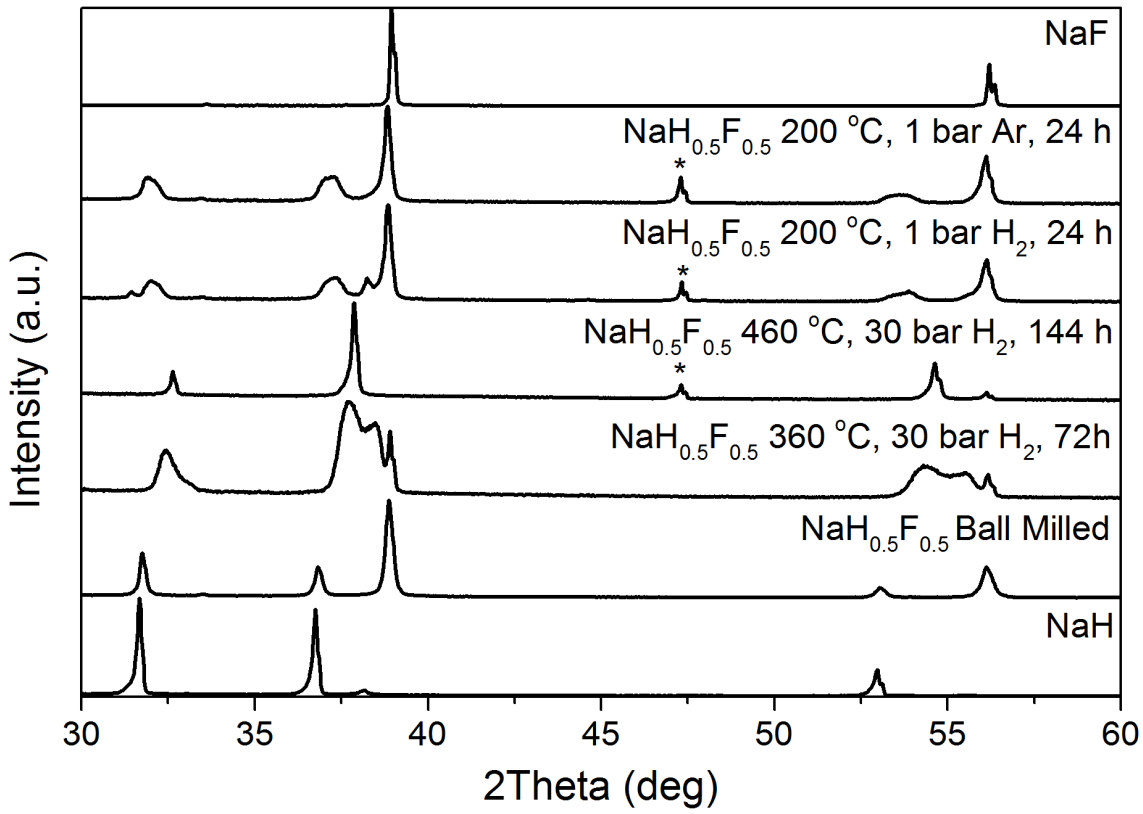

Fig. S2. XRD patterns of $NaH_{0.5}F_{0.5}$ mixtures annealed at various temperatures and atmospheres. * = Si internal standard. $\lambda = CuK_{\alpha}$.

Table S3. Lattice Parameters of $NaH_{0.5}F_{0.5}$ mixtures annealed at various temperatures and atmospheres. ESD's derived by Rietveld refinement are in parentheses.

Sample	**Lattice Parameter (Å)**	**Wt.% (%)**	**Composition[+]**
NaH (as supplied)*	4.88166(5)	95.44(1)	NaH
	NA	3.221(8)	$NaOH^{I-}$
	NA	1.381(2)	Na
NaF (as supplied)*	4.633222(4)	100	NaF
NaH + NaF (50:50 mol.%) Ball milled*	4.8805(2)	27.5(2)	NaH
	NA	5.1(3)	$NaOH^{I-}$
	4.6326(1)	67.3(3)	NaF
30 bar H_2, 300 °C, 72 h*	4.7647(4)	53.6(6)	$NaH_{0.57}F_{0.43}$
	4.6865(4)	39.7(6)	$NaH_{0.25}F_{0.75}$
	4.6266(2)	6.7(4)	NaF
30 bar H_2, 460 °C, 114 h	4.74362(8)	100	$NaH_{0.5}F_{0.5}$
1 bar H_2, 200 °C, 24 h	4.810(1)	29(1)	$NaH_{0.76}F_{0.24}$
	4.856(1)	4.2(9)	$NaH_{0.95}F_{0.05}$
	4.6317(1)	44(1)	NaF
	NA	14.4(5)	$NaOH^{I-}$
	NA	5.2(1)	Si
1 bar H_2, 200 °C, 24 h	4.8552(4)	13.2(6)	$NaH_{0.95}F_{0.05}$
	4.6334(1)	43.7(6)	NaF
	4.8171(5)	28.2(7)	$NaH_{0.79}F_{0.21}$
	NA	6.0(5)	$NaOH^{I-}$
	NA	8.8(1)	Si

[+]Composition determined by Eq 1 in main text. * No internal Si standard used for determination of lattice parameters so compositions may not be entirely accurate. [I-] Presence of NaOH is most likely due to air exposure through PMMA XRD sample holder.

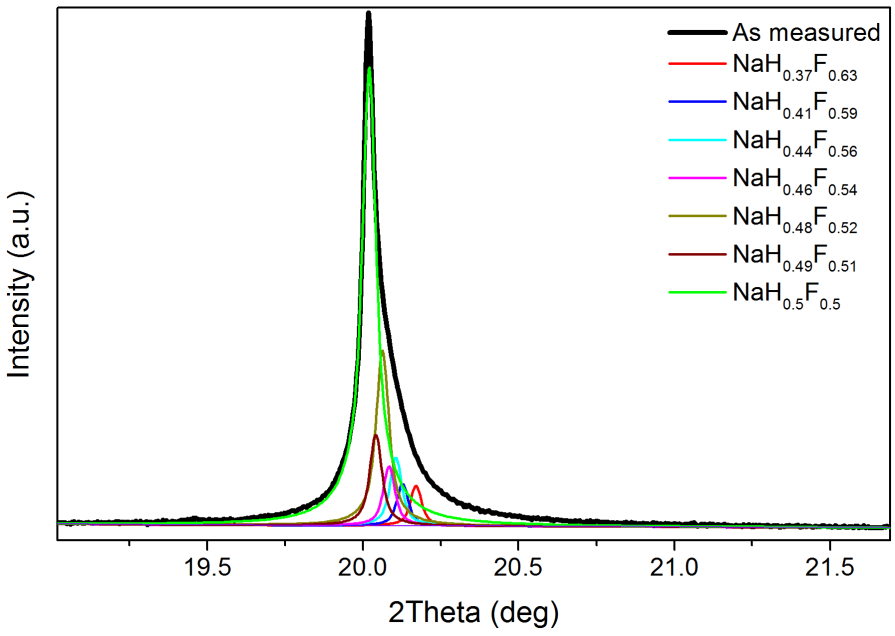

Fig. S3. SR-XRD patterns of $NaH_{0.5}F_{0.5}$ between 18 and 22° 2Θ along with profiles fitted during Reitveld refinement showing composition. λ = 0.824890 Å, T = 27 °C.

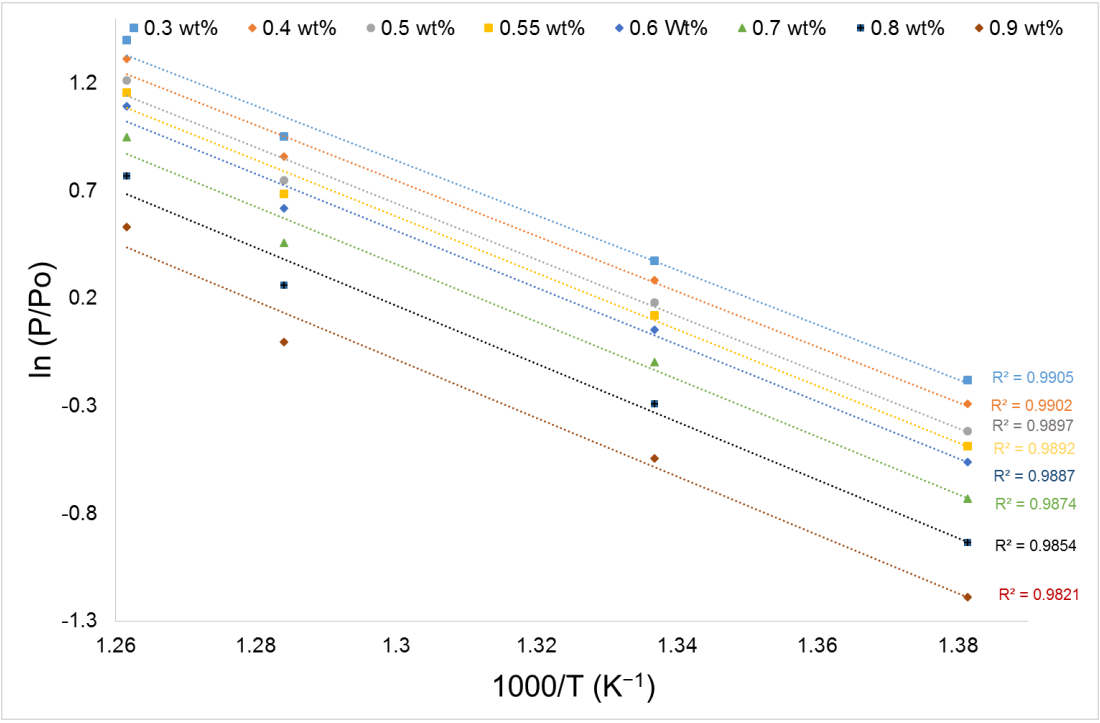

Fig. S4. Van't Hoff plots of $NaH_{0.5}F_{0.5}$ determined over the entire decomposition process by numerical fitting of the PCI data (method 2).

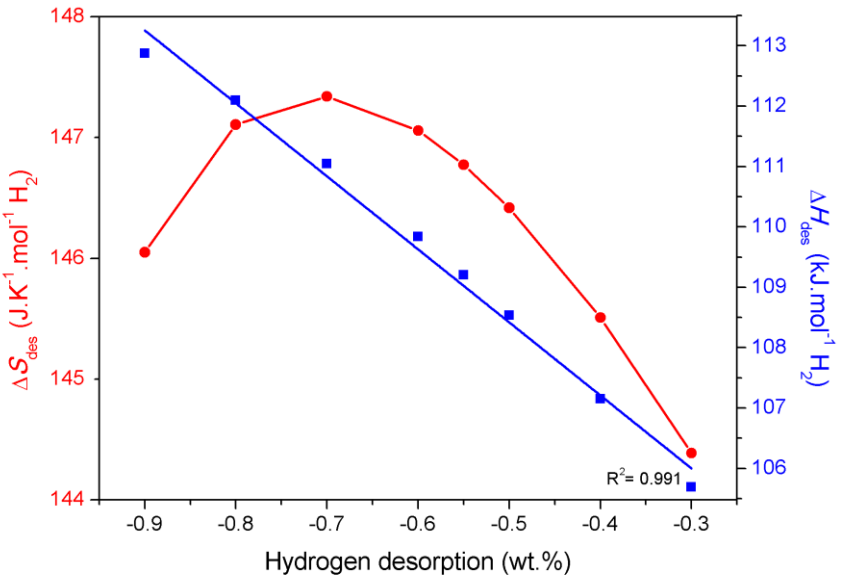

Fig. S5. Variation of Δ*H* and Δ*S* over the duration of Hydrogen desorption determined by numerical fitting of the PCI data (method 2).

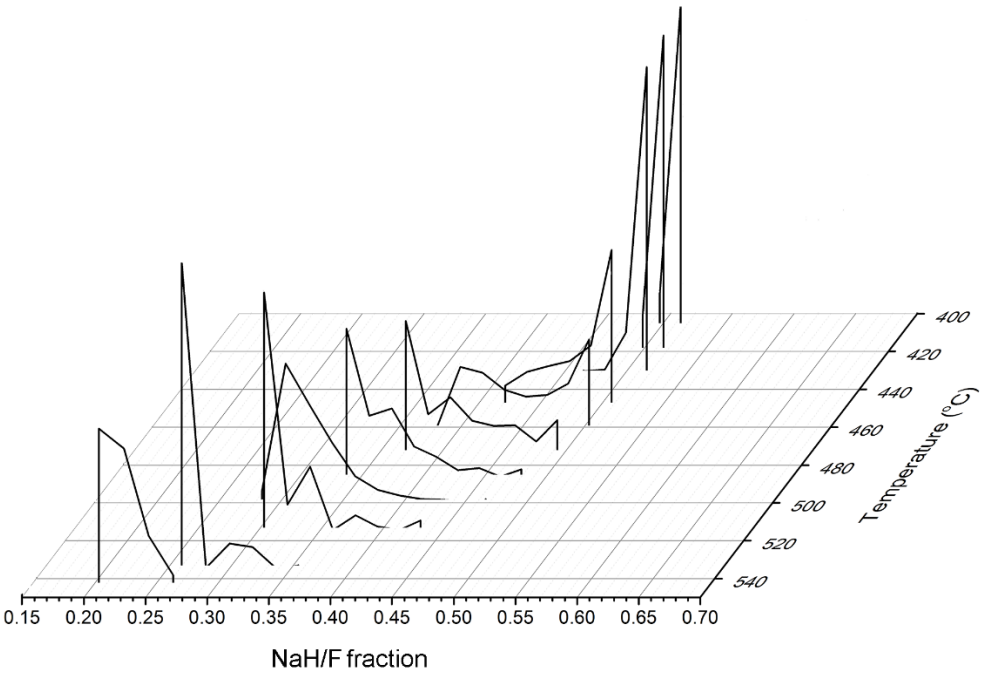

Fig. S6. Composition of $NaH_{0.5}F_{0.5}$ as a function of temperature measured by *in situ* XRD during heating.∫

∫$NaH_{1-x}F_x$ compositions were determined by correlation of the refined lattice parameters of data at specific temperatures. The thermal expansion of NaH, $NaH_{0.95}F_{0.05}$, $NaH_{0.85}F_{0.15}$, $NaH_{0.7}F_{0.3}$, $NaH_{0.5}F_{0.5}$ and NaF were measured by *in situ* XRD. The lattice parameters of each composite at a specific temperature were then treated by a quadratic expression to allow determination of any $NaH_{1-x}F_x$ composition at any temperature.

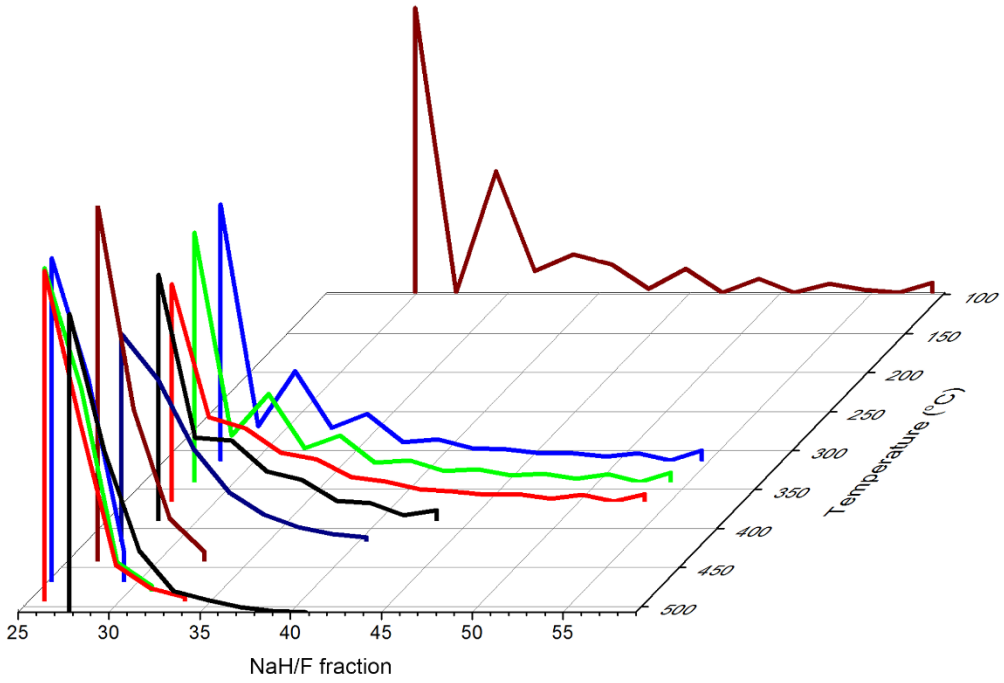

Fig. S7. Composition of $NaH_{0.5}F_{0.5}$ as a function of temperature measured by *in situ* XRD during cooling.∫